PYROXENE SPECTROSCOPY: PROBING COMPOSITION AND THERMAL HISTORY OF THE LUNAR SURFACE . R. L. Klima[1], C. M. Pieters[1] and M. D. Dyar[2], [1]Department of Geological Sciences, Brown University, Providence RI (Rachel_Klima@brown.edu), [2]Department of Astronomy, Mount Holyoke College, South Hadley, MA.

Introduction: Pyroxene is one of the most common and spectrally distinctive minerals on the lunar surface. Despite decades of research, the amount of mineralogical and compositional information that can be inferred from a remotely-detected pyroxene is limited. This is in part due to the complexity of the pyroxene mineral group. This complexity, however, contains a wealth of information about the composition and thermal history of the host rock. We report here the results of an extensive study of synthetic pyroxenes, of which the exact composition, thermal history, and site occupancy are known. These pyroxenes, which contain only the primary octahedral cations Ca^{2+}, Fe^{2+} and Mg^{2+}, allow us to describe the spectral behavior of 'pure' pyroxenes, providing a foundation for interpreting the causes of spectral deviations from these trends in natural samples. We further examine the spectra of eight pyroxenes separated from Apollo 15 and 17 samples that have been petrographically characterized by the Lunar Rock and Mineral Characterization Consortium (LRMCC) [1] in the context of these pyroxenes. These results will enhance quantitative analyses of new hyperspectral data being collected by the M^3 instrument on Chandrayaan-1 and the Spectral Profiler instrument on Kaguya.

Background: Two strong absorption bands near 1 and 2 μm, which result from crystal field transitions of Fe^{2+} in the pyroxene crystal, dominate the pyroxene near-infrared (NIR) spectrum (Fig. 1). The positions and shapes of these absorption bands are a result of the bulk composition, texture, and cooling history of the pyroxene. Previous research has focused primarily on understanding the effect of Fe^{2+}, Mg^{2+} and Ca^{2+} on these major absorption bands to deduce major element composition from remotely detected spectra [e.g., 2, 3-9]. However, it is recognized that minor elements often result in a distortion of the expected positions of the bands [e.g., 4, 6, 10]. Additionally, disordering of Fe^{2+} between the two octahedral pyroxene crystallographic sites (more Fe^{2+} in the smaller M1 site than expected) is reflected in the NIR spectrum[11, 9, 12].

Shown in Fig. 2 is a plot of the Band 1 (1 μm) and Band 2 (2μm) centers for a series of natural pyroxenes measured by [2, 6]. Though the general trends are controlled by the amount of Fe^{2+} and Ca^{2+} in the pyroxene, pyroxenes with high amounts of minor elements such as Al^{3+} or Ti plot away from these trends. These trends also rely necessarily on natural terrestrial pyroxenes, many of which are lower in Fe^{2+} than the lunar pyroxenes and/or contain oxidized Fe or Ti.

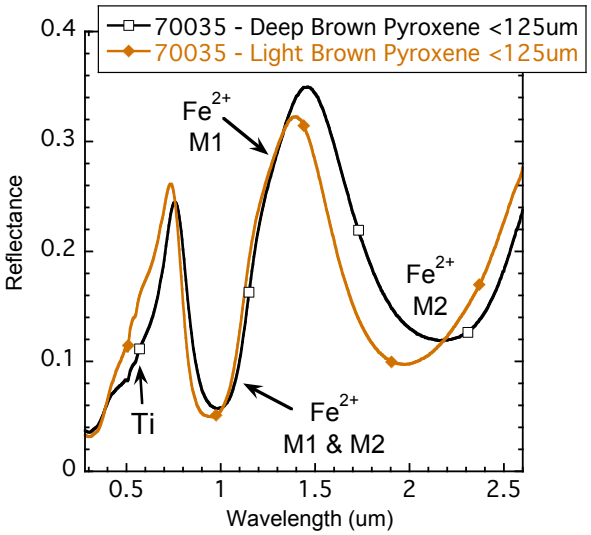

Fig. 1. Spectra of two pyroxenes from high-Ti mare basalt 70035. The deep-brown pyroxene is an augite containing greater amounts of Ti^{3+} than the light-brown (mostly pigeonite but some augite) pyroxene. Absorption bands due to Fe^{2+} in the M1 and M2 sites are observed at 1 μm, 1.2 μm and 2 μm.

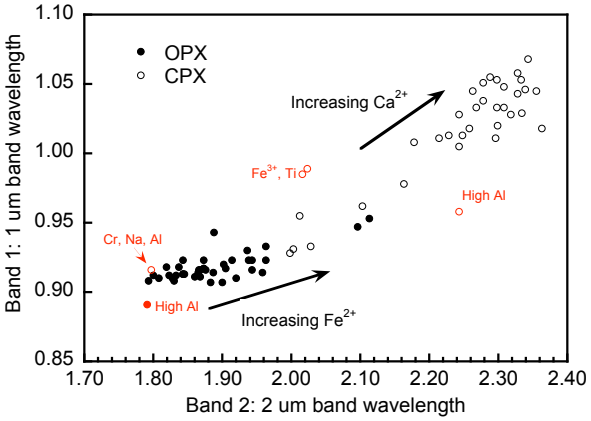

Fig. 2. Band 1 and 2 centers for a suite of natural pyroxenes, measured and analyzed by Adams [1974] and Cloutis and Gaffey [1991].

Preliminary Results: The synthesis and analyses procedures for the suite of synthetic pyroxenes are detailed in [13, 9]. Our current investigation of pure quadrilateral synthetic pyroxenes suggests that the composition and structure of the pyroxene control the placement of the 1 and 2 μm bands [9]. Deconvolution

of synthetic pyroxenes into component absorption bands has been used to isolate the crystal field absorptions. These model-derived band centers are compared with the band centers measured for naturally occurring pyroxenes by previous studies in Fig. 3. When a pyroxene is low in Ca^{2+}, the 1 and 2 μm band positions are closely coupled, suggesting that adding Fe^{2+} and Ca^{2+} to the pyroxene primarily affects the environment around M2 site. When the cation percentage of Ca^{2+} [$Ca^{2+}/(Ca^{2+}+Mg^{2+}+Fe^{2+})$] is greater than 30%, the 2 μm band becomes relatively stationary when compared to the 1 μm band, suggesting that Ca^{2+} is no longer significantly affecting the ligand environment around the M2 site, but *is* affecting that of the M1 site. With the framework laid out by the synthetic pyroxene studies, we can begin to evaluate how structural changes caused by minor elements affect the positions of the 1 and 2 μm pyroxene bands. Deviations from the observed trends should be coupled to the effect of commonly occurring minor elements on the M1 and/or M2 ligand environment(s).

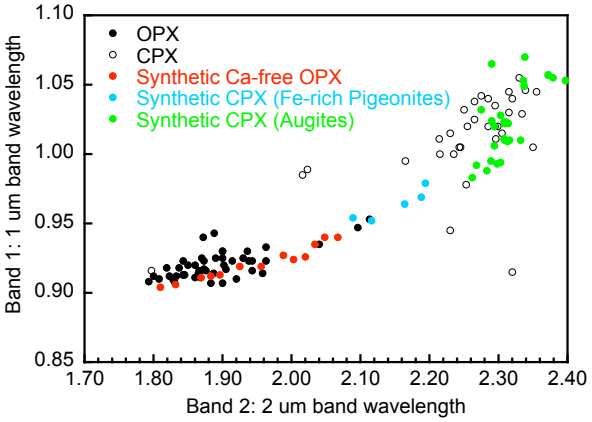

Fig. 3. Band centers of the synthetic pyroxenes compared with those of the pyroxenes from Fig. 2.

Lunar Pyroxenes: Eight lunar pyroxenes have been separated from four mare basalt samples for the LRMCC [1]. The relationship of the pyroxene spectra to the whole-rock spectra for these suites of samples is investigated in [14, 15]. Two of the basalts, 70017 and 70035, are high-Ti basalts containing pyroxenes that are enriched in Ti^{3+}.

Preliminary spectral modeling of the lunar pyroxene separates suggests that each separate contains some contribution of low and high-Ca pyroxene [16]. This is not unexpected, as the high and low Ca separates actually represent portions of extensively zoned larger pyroxene crystals [1]. An absorption near 0.65 μm is clearly visible in the more Ti-enriched Apollo 17 augites (Fig. 1). The band positions for models using 1 and 2 pyroxene solutions for each separate will be compared with the trends described by the synthetic pyroxenes. We will relate these results to the compositions of each of the pyroxene separates as measured by the LRMCC [1] to determine which spectral properties can be related to elevated amounts of Ti^{3+} and/or Al^{3+}.

Relevance to Lunar Science: Evidence from Apollo samples (and subsequent Lunar Prospector and Clementine data) suggests that the primary lunar crust, currently preserved in the highlands, evolved from plagioclase floatation on a crystallizing magma ocean [e.g., 17, 18]. Subsequent lunar volcanism, fueled by melting of the mafic residue, resulted in formation of the lunar Maria [19, 20, 18]. Though the general model of a lunar magma ocean is widely accepted, numerous questions remain concerning the composition of the lunar mantle and the origin of specific geochemically distinct groups such as the KREEP basalts and the Mg-rich suite.

The high spectral and spatial resolution imaging spectrometers M3 and Spectral Profiler are returning NIR data that will allow us to address these questions with a global view of the Moon. As the dominant Fe-bearing phase on the lunar surface, pyroxenes are key in extracting compositional information from these NIR spectra. Comparison with the synthetic pyroxene trends will allow us to identify the general bulk composition of lunar pyroxenes, and analysis of the spectra of lunar samples will allow us to relate strong deviations from the trends to enrichments in minor elements such as Al^{3+}, Ti^{3+}, or Cr^{3+}, which in turn enables us to address questions about the nature of the basalts' source composition.

Acknowledgements: We are extremely grateful to Don Lindsley and Allan Turnock for providing us the synthetic pyroxene samples. We also thank Takahiro Hiroi for his dedication and careful work in measuring these samples in RELAB. This work was supported by NASA grants #NNX07AP41G (CMP & RLK), #NNG05GG15G (CMP) and #NNG04GG12G (MDD). RELAB is a multiuser facility supported by NASA grant #NNG06GJ31G.

References: 1. Basu Sarbadhikari, A., et al. 2008. *LPSC XXXIX Abstract#1290*. 2. Adams, J.B., 1974. JGR, **79**(32): p. 4829. 3. Adams, J.B., 1975. in C.J. Karr, Ed., Academic Press Inc.: New York. p. 91. 4. Hazen, R.M., et al. 1978. in *LPSC IX*. 5. Cloutis, E.A. and M.J. Gaffey, 1991. Earth Moon and Planets, **53**(1): p. 11. 6. Cloutis, E.A. and M.J. Gaffey, 1991. JGR, **96**(E5): p. 22809. 7. Lucey, P.G., 1998I. JGR, **103**: p. 1703. 8. Denevi, B.W., et al., 2007. JGR, **112**(E05009). 9. Klima, R.L., et al., 2007. MAPS, **42**(2): p. 235. 10. Cloutis, E.A., 2002. JGR, **107**(E6). 11. Burns, R.G., et al., 1991, NASA #N92-10823: Washington, DC. p. 253. 12. Klima, R.L., et al., 2008. MAPS, **43**(10). 13. Turnock, A.C., et al., 1973. Am Min, **58**: p. 50. 14. Hiroi, T., et al. 2009. in *LPSC XL* Abstract #1723. 15. Isaacson, P.J., et al. 2009. in *LPSC XL* Abstract# 1821. 16. Klima, R. et al. 2008. LPSC XXXIX Abstract #1756. 17. Wood, J.A., et al. 1970. in *LPSC I*. 18. Shearer, C.K., et al., 2006. in B.L. Jolliff, et al., Editors., MSA: Chantilly. p. 365. 19. Warren, P.H., 1985. Ann Rev of Earth and Plan. Sci, **13**: p. 201. 20. Hess, P.C. and E.M. Parmentier, 1995I. EPSL, **134**: p. 501.